

Controlling light scattering and polarization by spherical particles with radial anisotropy

Y. X. Ni,¹ L. Gao,^{1,*} A. E. Miroshnichenko,² and C. W. Qiu³

¹Jiangsu Key Laboratory of Thin Films, Department of Physics, Soochow University, Suzhou 215006, China

²Nonlinear Physics Centre, Australian National University, Canberra, Australian Capital Territory 0200, Australia

³Department of Electrical and Computer Engineering, National University of Singapore, 4 Engineering Drive 3, Singapore 117576, Singapore

*leigao@suda.edu.cn

Abstract: Based on full-wave electromagnetic theory, we derive the zero-forward and zero-backward scattering conditions for radially anisotropic spheres within the quasi-static limit. We find that the near-field intensity can be tuned dramatically through the adjustment of the radial anisotropy, while the far-field light scattering diagrams are similar under the zero-forward or zero-backward scattering conditions. Generalized “Brewster’s angle” for anisotropic spheres is also derived, at which the scattering light is totally polarized. In addition, the high-quality polarized scattering wave and the tunable polarization conversion can be achieved for the radially anisotropic spheres.

© 2013 Optical Society of America

OCIS codes: (290.4020) Mie theory; (290.5850) Scattering particles; (160.1190) Anisotropic optical material; (260.5430) Polarization.

References and links

1. L. Rayleigh, “On the light from the sky, its polarization and color appendix,” *Philos. Mag.* **41**, 107–120 (1871).
2. G. Mie, “Contributions to the optics of turbid media, particularly colloidal metal solutions,” *Ann. Phys.* **25**, 377–445 (1908).
3. C. F. Bohren and D. R. Huffman, *Absorption and Scattering of Light by Small Particles* (Wiley, 1983).
4. M. Born and E. Wolf, *Principles of Optics: Electromagnetic theory of propagation, interference and diffraction of light*, 7th (expanded) ed. (Cambridge, 1999).
5. P. Bhatia and B. D. Gupta, “Fabrication and characterization of a surface plasmon resonance based fiber optic urea sensor for biomedical applications,” *Sens. Actuators B* **161**, 434–438 (2012).
6. T. Rindzevicius, Y. Alaverdyan, A. Dahlin, F. Hook, D. S. Setherland, and M. Kall, “Plasmonics sensing characteristics of single nanometric holes,” *Nano Lett.* **5**, 2335–2339 (2005).
7. S. Albaladejo, M. I. Marques, M. Laroche, and J. J. Sáenz, “Scattering forces from the curl of spin angular momentum of a light field,” *Phys. Rev. Lett.* **102**, 113602 (2009).
8. M. Nieto-Vesperinas, J. J. Sáenz, R. Gómez-Medina, and L. Chantada, “Optical forces on small magnetodielectric particles,” *Opt. Express* **18**, 11428–11443 (2010).
9. J. A. Gordon and R. W. Ziolkowski, “The design and simulated performance of a coated nano-particle laser,” *Opt. Express* **15**, 2622–2653 (2007).
10. J. B. Pendry, “Negative refraction makes a perfect lens,” *Phys. Rev. Lett.* **85**, 3966–3969 (2000).
11. Z. Liu, S. Durant, H. Lee, Y. Picus, N. Fang, Y. Xiong, C. Sun, and X. Zhang, “Far-field optical superlens,” *Nano Lett.* **7**, 403–408 (2007).
12. J. B. Pendry, D. Schurig, and D. R. Smith, “Controlling electromagnetic fields,” *Science* **312**, 1780–1782 (2006).
13. M. I. Tribelsky and B. S. Luk’yanchuk, “Anomalous light scattering by small particles,” *Phys. Rev. Lett.* **97**, 263902 (2006).

14. M. I. Tribelsky, S. Flach, A. E. Miroshnichenko, A. V. Gorbach, and Y. S. Kivshar, "Light scattering by a finite obstacle and Fano resonance," *Phys. Rev. Lett.* **100**, 043903 (2008).
15. Z. Liu, Z. Lin, and S. T. Chui, "Electromagnetic scattering by spherically negative-refractive-index particles: low frequency resonance and localization parameters," *Phys. Rev. E* **69**, 016609 (2004).
16. A. E. Miroshnichenko, "Non-Rayleigh limit of the Lorenz-Mie solution and suppression of scattering by spheres of negative refractive index," *Phys. Rev. A* **80**, 013808 (2009).
17. M. Kerker, D. S. Wang, and C. L. Giles, "Electromagnetic scattering by magnetic spheres," *J. Opt. Soc. Am.* **73**, 765–767 (1983).
18. B. García-Cámara, F. González, F. Moreno, and J. M. Saiz, "Exception for the zero-forward-scattering theory," *J. Opt. Soc. Am. A* **25**, 2875–2878 (2008).
19. B. García-Cámara, J. M. Saiz, F. González, and F. Moreno, "Nanoparticles with unconventional scattering properties: size effects," *Opt. Commun.* **283**, 490–496 (2010).
20. B. García-Cámara, R. Alcaraz de la Osa, J. M. Saiz, F. González, and F. Moreno, "Directionality in scattering by nanoparticles: Kerker's null-scattering conditions revisited," *Opt. Lett.* **36**, 728–730 (2011).
21. B. García-Cámara, F. Moreno, F. González, J. M. Saiz, and G. Videen, "Light scattering resonances in small particles with electric and magnetic properties," *J. Opt. Soc. Am. A* **25**, 327–334 (2008).
22. J. M. Geffrin, B. García-Cámara, R. Gómez-Medina, P. Albella, L. S. Froufe-Pérez, C. Eyraud, A. Litman, R. Vaillon, F. González, M. Nieto-Vesperinas, J. J. Sáenz, and F. Moreno, "Magnetic and electric coherence in forward- and back-scattered electromagnetic waves by a single dielectric subwavelength sphere," *Nat. Commun.* **3**, 1171 (2012).
23. Y. H. Fu, A. I. Kuznetsov, A. E. Miroshnichenko, Y. F. Yu, and B. Luk'yanchuk, "Directional visible light scattering by silicon nanoparticles," *Nat. Commun.* **4**, 1527 (2013).
24. S. Person, M. Jain, Z. Lapin, J. J. Sáenz, G. Wicks, and L. Novotny, "Demonstration of zero optical backscattering from single nanoparticles," <http://arxiv.org/abs/1212.2793v1>.
25. J. Roth and M. J. Digman, "Scattering and extinction cross sections for a spherical particle coated with an oriented molecular layer," *J. Opt. Soc. Am.* **63**, 308–311 (1973).
26. V. L. Sukhorukov, G. Meedt, M. Kurschner, and U. Zimmermann, "A single-shell model for biological cells extended to account for the dielectric anisotropy of the plasma membrane," *J. Electrostat.* **50**, 191–204 (2001).
27. T. Ambjörnsson, G. Mukhopadhyay, S. P. Apell, and M. Kall, "Resonant coupling between localized plasmons and anisotropic molecular coatings in ellipsoidal metal nanoparticles," *Phys. Rev. B* **73**, 085412 (2006).
28. L. Gao, T. H. Fung, K. W. Yu, and C. W. Qiu, "Electromagnetic transparency by coated spheres with radial anisotropy," *Phys. Rev. E* **78**, 046609 (2008).
29. L. Gao and X. P. Xu, "Second- and third-harmonic generations for a nondilute suspension of coated particles with radial dielectric anisotropy," *Eur. Phys. J. B* **55**, 403–409 (2007).
30. X. Fan, Z. Shen, and B. S. Luk'yanchuk, "Huge light scattering from anisotropic spherical particles," *Opt. Express* **18**, 24868–24880 (2010).
31. C. W. Qiu and B. S. Luk'yanchuk, "Peculiarities in light scattering by spherical particles with radial anisotropy," *J. Opt. Soc. Am. A* **25**, 1623–1628 (2008).
32. Y. X. Ni, L. Gao, A. E. Miroshnichenko, and C. W. Qiu, "Non-Rayleigh scattering behavior for anisotropic Rayleigh particles," *Opt. Lett.* **37**, 3390–3392 (2012).
33. H. L. Chen and L. Gao, "Anomalous electromagnetic scattering from radially anisotropic nanowires," *Phys. Rev. A* **86**, 033825 (2012).
34. J. M. Hao, Y. Yuan, L. X. Ran, T. Jiang, J. A. Kong, C. T. Chan, and L. Zhou, "Manipulating electromagnetic wave polarizations by anisotropic metamaterials," *Phys. Rev. Lett.* **99**, 063908 (2007).
35. B. S. Luk'yanchuk and C. W. Qiu, "Enhanced scattering efficiencies in spherical particles with weakly dissipating anisotropic materials," *Appl. Phys. A* **92**, 773–776 (2008).
36. A. Alù and N. Engheta, "How does zero forward-scattering in magnetodielectric nanoparticles comply with the optical theorem," *J. Nanophoton.* **4**, 041590 (2010).
37. C. Argyropoulos, P. Y. Chen, F. Monticone, G. D'Aguanno, and A. Alù, "Nonlinear plasmonic cloaks to realize giant all-optical scattering switching," *Phys. Rev. Lett.* **108**, 263905 (2012).
38. M. Nieto-Vesperinas, R. Gómez-Medina, and J. J. Sáenz, "Angle-suppressed scattering and optical forces on sub-micrometer dielectric particles," *J. Opt. Soc. Am. A* **28**, 54–60 (2011).
39. R. Gómez-Medina, B. García-Cámara, I. Suárez-Lacalle, F. González, F. Moreno, M. Nieto-Vesperinas, J. J. Sáenz, "Electric and magnetic dipolar response of germanium nanospheres: interference effects, scattering anisotropy, and optical forces," *J. Nanophoton.* **5**, 053512 (2011).
40. C. E. Dean and P. L. Marston, "Critical angle light scattering from bubbles: an asymptotic series approximation," *Appl. Opt.* **30**, 4764–4776 (1991).
41. B. García-Cámara, F. González, F. Moreno, "Linear polarization degree for detecting magnetic properties of small particles," *Opt. Lett.* **35**, 4084–4086 (2010).

1. Introduction

The light scattering from small particles has long been a topic of great interest [1–4]. For a homogeneous sphere with arbitrary size, the full-wave electromagnetic theory was established to investigate the light scattering [2]. Nowadays, the interest in this field has been increased even more due to its potential applications in subwavelength optics, information processing and nanotechnologies.

Recently, technological success in the fabrication of nanostructured materials has led to an emergence of growing field of nanophotonics. Nanostructured materials possess unique optical, electric and magnetic properties compared to bulk materials, they have many potential applications in biomedical sciences [5,6], optical forces and trapping [7,8], and high-resolution optical imaging [9]. On the other hand, with the prosperous progress in the engineered materials (known as “metamaterials”), especially in the negatively refractive materials, much effort was devoted to these artificial materials for their interesting and novel properties such as perfect lens [10,11] and electromagnetic cloaking [12]. In this connection, almost every corner of electrodynamics theory was reexamined and many unusual phenomena were observed. For instance, Anomalous light scattering and Fano resonance were revealed from nanospheres with low dissipation rate [13,14]. Non-Rayleigh limits for the scattering efficiency Q_{sca} from the small particles made of metamaterials were demonstrated such as $Q_{sca} \sim 1/q^2$ (size parameter $q = 2\pi a/\lambda$, where a is the radius of the sphere and λ is the illuminating wavelength) or $Q_{sca} \sim const$ under certain conditions [15,16]. On the other hand, thirty years ago, Kerker *et al.* showed that the forward scattering and backward scattering can be almost suppressed if the dielectric and magnetic properties of the isotropic scatters satisfy certain relations [17]. García-Cámara *et al.* renewed Kerker’s zero-forward scattering condition [18–20] and studied the Mie resonance of light scattering by small particles with negative physical parameters [21]. More recently, Geffrin *et al.* [22] gave unambiguous experimental evidence of observing the zero-forward scattering, and experimental verifications of Kerker’s theoretical prediction in the optical wavelength range was reported [23,24]. Note that above investigations were valid for isotropic cases only.

In this paper, we would like to investigate the electromagnetic scattering from nanospheres with radial anisotropy. As a matter of fact, the majority of solid materials in nature are anisotropic, and radial anisotropy was indeed found in many nanostructures such as biological cells containing mobile charges and real phospholipid vesicles [25–27]. In addition, it was found that radial anisotropy plays an important role in the creation of electromagnetic cloaking of invisibility [12,28], and much interesting progress was also made for radially anisotropic structures [29–33]. Here, based on our previously derived scattering theory for radial anisotropy [28], we shall derive the zero-forward and zero-backward conditions for nanospheres when the radial anisotropy is taken into account. Furthermore, motivated by the investigation on the manipulation of the polarization states of electromagnetic waves through reflections by an anisotropic metamaterial slab [34], we take one step forward to study the polarization of the scattering wave from radially anisotropic spheres.

This paper is organized as follows. In Section 2, we review the general scattering theory of light scattering by radially anisotropic spherical particles. In Section 3, we study the light suppression in the forward and backward directions. Especially, the zero-forward and zero-backward scattering conditions for the radially anisotropic spheres are derived within the quasi-static limit. In Section 4, we illustrate the polarization of the light scattered by the spheres with radial anisotropy. Conclusions are made in Section 5.

2. Theoretical model

We consider the light scattering by a radially anisotropic sphere with radius a , surrounded by the free space with permittivity ϵ_0 and permeability μ_0 . Radial anisotropy means that the permittivity (or permeability) tensor is diagonal in spherical coordinates, and the element along the radial direction differs from the one along the tangential direction [25]. Here the relative permittivity and the permeability tensors are written in the spherical coordinates as, $\bar{\epsilon} = (\epsilon_r \hat{r}\hat{r} + \epsilon_t \hat{\theta}\hat{\theta} + \epsilon_t \hat{\phi}\hat{\phi})$ and $\bar{\mu} = (\mu_r \hat{r}\hat{r} + \mu_t \hat{\theta}\hat{\theta} + \mu_t \hat{\phi}\hat{\phi})$. For simplicity, we assume the polarized wave with unit amplitude to be $E_i = \hat{e}_x \exp(ik_0 z)$ with $k_0 = \omega \sqrt{\epsilon_0 \mu_0}$. We can generalize the Lorenz-Mie scattering theory [3,4] to study light scattering by spherical particle with radial anisotropy through Debye potentials. After some algebraic manipulations, we can obtain the electric and magnetic scattering coefficients [28,35],

$$a_n = \frac{\sqrt{\epsilon_t} \psi'_n(q) \psi_{v_n}(mq) - \sqrt{\mu_t} \psi_n(q) \psi'_{v_n}(mq)}{\sqrt{\epsilon_t} \xi'_n(q) \psi_{v_n}(mq) - \sqrt{\mu_t} \xi_n(q) \psi'_{v_n}(mq)}, \quad (1)$$

$$b_n = \frac{\sqrt{\epsilon_t} \psi_n(q) \psi'_{\gamma_n}(mq) - \sqrt{\mu_t} \psi'_n(q) \psi_{\gamma_n}(mq)}{\sqrt{\epsilon_t} \xi_n(q) \psi'_{\gamma_n}(mq) - \sqrt{\mu_t} \xi'_n(q) \psi_{\gamma_n}(mq)}, \quad (2)$$

where $m = \sqrt{\epsilon_t} \sqrt{\mu_t}$ is the refractive index of the sphere relative to vacuum, $q = k_0 a$ is the size parameter, $\psi_n(x)$ and $\xi_n(x)$ are the Ricatti-Bessel functions. The primes indicate differentiation with respect to the entire argument of the corresponding functions. From Eqs. (1) and (2), we find that all the information on the particle anisotropy is presented by the orders of spherical Bessel functions,

$$v_n = \sqrt{n(n+1)Ae + \frac{1}{4} - \frac{1}{2}} \quad \text{and} \quad \gamma_n = \sqrt{n(n+1)Am + \frac{1}{4} - \frac{1}{2}}, \quad (3)$$

where $Ae = \epsilon_t / \epsilon_r$ and $Am = \mu_t / \mu_r$ are, respectively, the electric and magnetic anisotropy ratios. For the isotropic case, $Ae = Am = 1$, Eqs. (1) and (2) are naturally reduced to the exact formulae of Mie theory.

The scattered radiant intensity I is composed of two polarized components [17],

$$I = I_1 + I_2 = \frac{\lambda^2}{4\pi^2 r^2} \left\{ |S_\perp|^2 \sin^2 \phi + |S_\parallel|^2 \cos^2 \phi \right\}, \quad (4)$$

where I_1 and I_2 are the two polarized components of the scattered intensity when the incident electric field vector is perpendicular (TE) and parallel (TM) to the scattering plane, which contains the incident direction and the direction of the scattered wave. In addition, λ is the incident wavelength, r is the distance to the observer, and ϕ is the angle between the electric vector of the incident wave and the scattering plane. And the amplitude functions S_\perp and S_\parallel are defined as,

$$S_\perp = \sum_{n=1}^{\infty} \frac{2n+1}{n(n+1)} [a_n \pi_n(\cos \theta) + b_n \tau_n(\cos \theta)], \quad (5)$$

$$S_\parallel = \sum_{n=1}^{\infty} \frac{2n+1}{n(n+1)} [a_n \tau_n(\cos \theta) + b_n \pi_n(\cos \theta)], \quad (6)$$

where the angular functions $\pi_n = P_n^1(\cos \theta) / \sin \theta$ and $\tau_n = dP_n^1(\cos \theta) / d\theta$, with θ being the angle between the forward and scattering directions. Note that there are two special directions such as 0° and 180° at which the scattering does not depend on the input polarization. In this

connection, we can write the reflection (backward, $\theta = 180^\circ$) R and transmission (forward, $\theta = 0^\circ$) T amplitudes,

$$R = S_{\perp,\parallel}(180^\circ) = \sum_{n=1}^{\infty} \frac{2n+1}{n(n+1)} (a_n - b_n), \quad (7)$$

$$T = S_{\perp,\parallel}(0^\circ) = \sum_{n=1}^{\infty} \frac{2n+1}{n(n+1)} (a_n + b_n). \quad (8)$$

3. Conditions for suppression of the scattering intensity

As we know for the magnetic or nonmagnetic small spheres with large values of permittivity, the scattered radiant intensity may be either preferentially back or forward scattered [17]. This asymmetry originally arises from the interference between the electric and magnetic dipole modes. It is evident that the scattering in the backward direction can be totally suppressed (i. e. $R = 0$) for the scattering coefficients satisfying $a_n = b_n$, whereas the scattering in the forward direction can be totally suppressed (i. e. $T = 0$) when $a_n = -b_n$.

In the long-wave ($q = 2\pi a/\lambda \ll 1$) and low-frequency ($mq \ll 1$) limit, the higher terms for $n > 1$ are so small that can be neglected, and the scattering efficiency is mainly characterized by the first two scattering coefficients a_1 and b_1 , which represent the dipole contributions. Correspondingly, the Riccati-Bessel functions with small arguments for $n = 1$ and non-integer order ν are approximately to be,

$$\begin{aligned} \psi_1(x) &\sim \frac{x^2}{3} - \frac{x^4}{30}, & \xi_1(x) &\sim -\frac{i}{x} - \frac{ix}{2} + \frac{x^2}{3}, \\ \psi_\nu(x) &\sim \frac{\sqrt{\pi}}{\Gamma(\nu + \frac{3}{2})} \left(\frac{x}{2}\right)^{\nu+1} - \frac{\sqrt{\pi}}{\Gamma(\nu + \frac{5}{2})} \left(\frac{x}{2}\right)^{\nu+3}. \end{aligned} \quad (9)$$

Then, the scattering coefficients a_1 and b_1 with small arguments are,

$$a_1 \simeq \frac{2\varepsilon_t - (\nu_1 + 1)}{3i(\varepsilon_t + \nu_1 + 1)} q^3 \quad \text{and} \quad b_1 \simeq \frac{2\mu_t - (\gamma_1 + 1)}{3i(\mu_t + \gamma_1 + 1)} q^3. \quad (10)$$

As a consequence, we obtain the zero-backward and zero-forward scattering conditions for small particles with radial anisotropy,

$$\frac{\varepsilon_t}{\nu_1 + 1} = \frac{\mu_t}{\gamma_1 + 1} \quad \text{and} \quad \frac{\varepsilon_t}{\nu_1 + 1} = \frac{2(\gamma_1 + 1) - \mu_t}{4\mu_t + (\gamma_1 + 1)}. \quad (11)$$

Here we would like to mention that Eq. (11) is reduced to Kerker's conditions for the isotropic case with $\nu_1 = \gamma_1 = 1$. Actually, zero-forward scattering intensity cannot be exactly obtained under the zero-forward scattering condition. The forward scattering intensity just leads to a minimum, and its magnitude is much smaller than the scattering in all other directions. The reason is that the zero-forward scattering condition is derived under the quasi-static limit, and the higher-order scattering coefficients (i.e. a_2, b_2, \dots), which definitely exist, have been omitted. In this sense, the overall scattering from the sphere is indeed low and the higher-order components of the forward scattering takes into account the extinction from the sphere, and then the optical theorem (the extinction cross section is proportional to the scattering amplitude in the forward direction) is satisfied [36]. In addition, there is an exception for zero-forward scattering when $\varepsilon_t = -(\nu_1 + 1)$ [we get $\mu_t = -(\gamma_1 + 1)$ with the condition for zero-forward scattering], at which the localized surface plasmon resonances are excited [18].

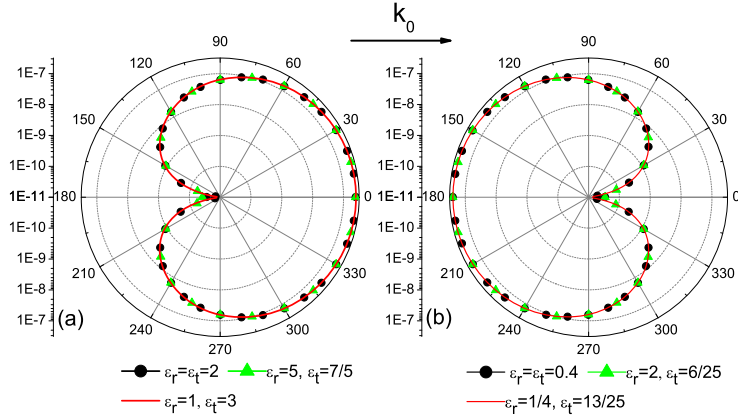


Fig. 1. Scattering intensity (logarithmic scale) as a function of the scattering angle calculated by full-wave scattering theory for spherical particles with $q = 0.1$, $\mu_r = \mu_t = 2$ when they are illuminated from left by a TM-polarized incident wave. The physical parameters satisfy either zero-backward scattering condition (a) or zero-forward scattering condition (b).

Figure 1 shows the far-field scattering diagrams of spherical particles with different radial anisotropies under zero-backward and zero-forward scattering conditions, illuminated by the TM-polarized incident light (under the zero-backward or zero-forward conditions, the results for TE-polarized wave are almost the same as those for TM one). If the physical parameters satisfy the first condition in Eq. (11), the backward scattering intensity is almost zero, as expected [see Fig. 1(a)]. On the other hand, the scattering diagram shows near zero forward scattering intensity [see the black solid line in Fig. 1(b)], when the parameters are chosen to satisfy the second condition in Eq. (11). We note that when the radial anisotropy in the permittivity is taken into account, the scattering diagrams keep invariant under the zero-forward (or backward) scattering conditions. Actually, for the given isotropic permeability $\mu_r = \mu_t = 2$, the scattering coefficient b_1 is fully fixed. Moreover, under the zero-forward (or backward) scattering condition, one yields $a_1 = -b_1$ (or $a_1 = b_1$) no matter what the anisotropic permittivities are chosen. As a consequence, the scattering intensity, determined mainly by the first two scattering coefficients a_1 and b_1 , is almost independent of the radial anisotropy.

In order to show how the scattered wave evolves from the near- to far-fields and how they are correlated, we calculate the total near-field intensity around the anisotropic particles under the zero-backward and zero-forward scattering conditions for various radial anisotropy in the permittivity, as shown in Figs. 2 and 3. From Fig. 2 (the zero-backward scattering condition holds), we can observe that the electromagnetic scattering is inhibited in the backward direction [see Figs. 2(a), 2(c) and 2(e)] and the modulus of the electric field is relatively large in the forward direction. On the contrary, under zero-forward scattering condition, we really observe that the electric field is suppressed in the forward direction (see Fig. 3). All these behavior coincides well with far-field scattering diagrams (see Fig. 2). To one's interest, although the introduction of the radial anisotropy in the permittivity has little influence on the scattering diagram, it leads to great modification in the local field distributions around the anisotropic particles. For instance, when the electric anisotropy ratio $A_e < 1$ [see Figs. 2(c) and 2(d)], the electric field is greatly enhanced when compared with the isotropic case [see Figs. 2(a) and 2(b)]. And the field is divergent at the center of the spheres. However, when $A_e > 1$ [see Figs. 2(e) and 2(f)], the internal field is found to be reduced considerably in comparison with the

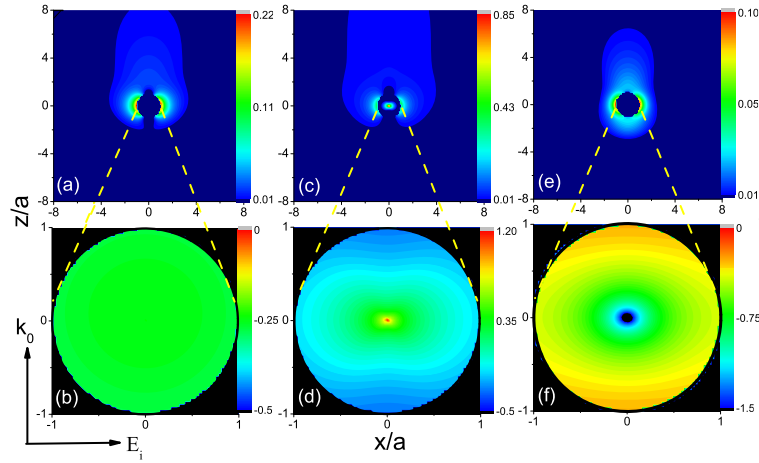


Fig. 2. Distribution of the total near-field intensity ($\log_{10}|E|$) calculated by full-wave scattering theory for the sphere with $q = 0.6$, $\mu_r = \mu_t = 2$ under the zero-backward scattering condition: $\epsilon_r = \epsilon_t = 2$ for (a) and (b), $\epsilon_r = 5$, $\epsilon_t = 7/5$ for (c) and (d), $\epsilon_r = 1$, $\epsilon_t = 3$ for (e) and (f). Note that (a), (c), (e): show the fields both inside and outside the spheres, whereas (b), (d), (f) show the fields inside the spheres only.

isotropic case, and is almost zero in the center of the spherical particle. The divergence and the vanish behavior in the center of spherical particles for different radial anisotropy under the zero-backward scattering condition is also observed (not shown here), and can be well understood within the quasi-static approximation [29]. It is interesting that for an observer sitting at the backward of the sphere, the fields are uniformly boosted all across the anisotropy we studied, but for an observer just inside the core, the fields can drastically change from almost zero to infinity [37]. Therefore, through the adjustment of the radial anisotropy, one can still enhance or weaken the local field inside the particles while keeping the scattering diagram almost invariant.

As suggested in [20] and [36], in deriving the zero-backward and zero-forward scattering conditions, one can take into account the radiative correction so as to satisfy the power conservation requirements. In this connection, the scattering coefficients a_1 and b_1 should be modified by,

$$a_1 \simeq \frac{1}{1 + \frac{3i(\epsilon_t + \nu_1 + 1)}{[2\epsilon_t - (\nu_1 + 1)]q^3}} \quad \text{and} \quad b_1 \simeq \frac{1}{1 + \frac{3i(\mu_t + \gamma_1 + 1)}{[2\mu_t - (\gamma_1 + 1)]q^3}}. \quad (12)$$

Then, the condition for zero-backward scattering is found to be the same as the first one in Eq. (11), while the condition for the zero-forward scattering is revised to be

$$\frac{\epsilon_t}{\nu_1 + 1} = \frac{3[2(\gamma_1 + 1) - \mu_t] - 2iq^3[2\mu_t - (\gamma_1 + 1)]}{3[4\mu_t + (\gamma_1 + 1)] - 4iq^3[2\mu_t - (\gamma_1 + 1)]}. \quad (13)$$

Similarly, Eq. (13) is reduced to the modified Kerker's condition [20] when $\nu_1 = \gamma_1 = 1$ for the isotropic case. In order to fulfill Eq. (13), at least one of the anisotropic parameters should be complex with negative imaginary part if other parameters are real. The negative imaginary part of $\epsilon_{r(t)}$ or $\mu_{r(t)}$ may result in negative absorption cross section or amplification cross section. The scatters with such a property are known as gain (active) objects. On the contrary, for usual passive spheres whose imaginary parts of the permeabilities and/or permittivities are positive, the corresponding electric or magnetic polarizability cannot have opposite sign to each other [36, 38, 39], and hence the zero-backward scattering condition is not fulfilled.

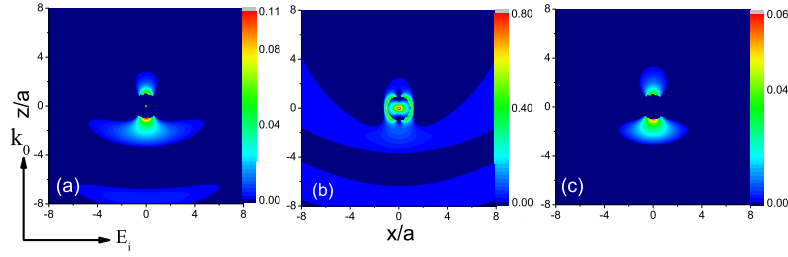


Fig. 3. Distribution of the total near-field intensity ($\log_{10}|E|$) calculated by full-wave scattering theory for the spheres with $q = 0.6$, $\mu_r = \mu_t = 2$ under the zero-forward scattering condition: $\epsilon_r = \epsilon_t = 0.4$ for (a), $\epsilon_r = 2$, $\epsilon_t = 6/25$ for (b), and $\epsilon_r = 1/4$, $\epsilon_t = 13/25$ for (c).

4. The polarization of the scattering wave

It is known that the polarization degree of the scattered wave from the isotropic particles provides us an alternative way for determining the physical parameters of the particles [40, 41]. In this section, we would like to study the polarization of the scattering wave from the anisotropic particles.

For an incident linearly polarized plane wave, the scattered wave from spherically anisotropic particle may have two polarized components (named as TE and TM). Especially, when the amplitude function S_{\perp} or S_{\parallel} equals zero, the scattering light will be totally polarized. The angle at which S_{\perp} (or S_{\parallel}) equals zero is defined as the generalized Brewster's angles for the sphere [16]. In the quasi-static limit, we obtain the analytical solution for the conditions to get the completely polarized wave,

$$\cos \theta_{\perp} = -\frac{(2\epsilon_t - (\nu_1 + 1))(\mu_t + (\gamma_1 + 1))}{(2\mu_t - (\gamma_1 + 1))(\epsilon_t + (\nu_1 + 1))}, \quad \cos \theta_{\parallel} = \frac{1}{\cos \theta_{\perp}}, \quad (14)$$

where θ_{\perp} (when $S_{\perp} = 0$) and θ_{\parallel} (when $S_{\parallel} = 0$) refer to the "Brewster's angles" for spherical particles with radial anisotropy. Moreover, the degree of polarization P of the scattered light is expressed as,

$$P = \frac{|S_{\perp}|^2 - |S_{\parallel}|^2}{|S_{\perp}|^2 + |S_{\parallel}|^2}. \quad (15)$$

It is evident that in the quasi-static limit, when the angle of incidence equals the Brewster's angle, P shall be 1 or -1 , indicating totally TE- or TM-polarized scattering light. On the other hand, for the spheres with large size parameters, we can directly resort to our generalized formalism Eqs. (5) and (6) with Eqs. (1) and (2) to present the numerical results. In Fig. 4, we plot the polarization diagram and P versus θ with $q = 0.5$ for different anisotropic permeabilities and permittivities. The following features are clearly noted: (1) The polarization can be nearly 1 or -1 , that is to say, totally polarized, when we adjust the electric and magnetic anisotropy ratios suitably; (2) Either TE-polarized scattering wave (see the blue short dashed and olive dash-dotted lines) or TM-polarized scattering wave (see the black solid and red dotted lines) is achieved from the radially anisotropic sphere; (3) Through tuning the anisotropy ratios it is possible to obtain high-quality polarized scattered waves in comparison with those from isotropic

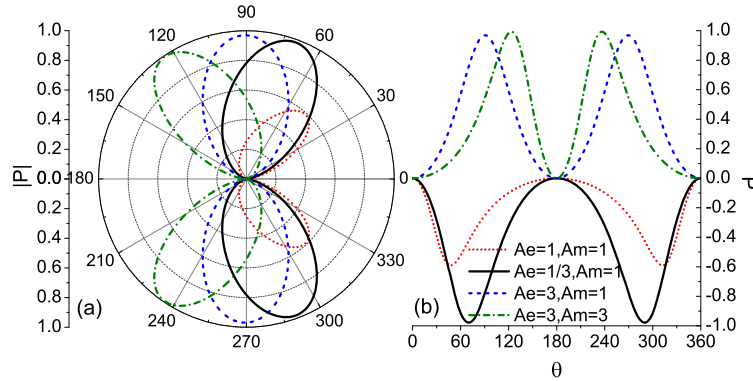


Fig. 4. The polar diagram of absolute value of polarization (a) and the degree of polarization versus θ (b) for $q = 0.5$, $\epsilon_r = -1$, $\mu_r = -5$, and for different radial anisotropy.

spheres. High-quality means the degree of polarization is larger and the range of “Brewster’s angles” are broader; (4) Tunable “Brewster’s angles” from forward ($0^\circ \sim 90^\circ$, see the black solid line) to backward ($90^\circ \sim 180^\circ$, see the dash-dotted olive line) directions can be achieved.

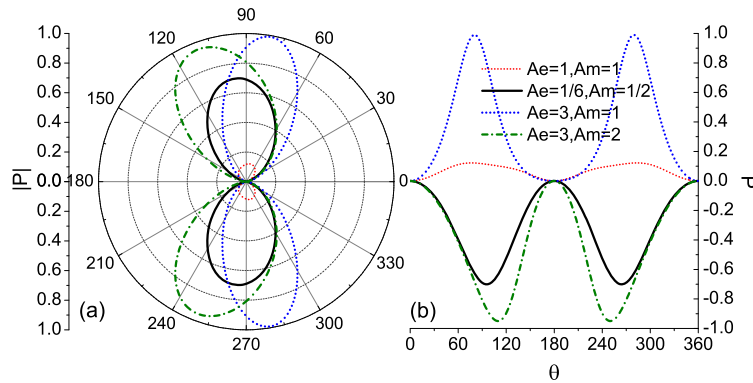


Fig. 5. Same as in Fig. 4 but with $q = 1$.

Figure 5 gives the results of the polarization patterns with $q = 1.0$. For the isotropic case ($A_e = 1$ and $A_m = 1$), increasing the size parameters while keeping the physical parameters unchanged will result in a lower degree of polarization (see the red short dotted lines in Figs. 4 and 5). However, as the radial anisotropy is taken into account, we can still get high-quality polarized scattering wave.

5. Conclusion

In summary, the light scattering of spherical particles with radially anisotropic permittivity and permeability is analyzed with the expanded Mie theory. We propose an analytical approach to obtain the zero-forward and zero-backward scattering intensity within the quasi-static approximation. Numerical results show that the near-field intensity can be enhanced or weakened by tuning the anisotropic permittivities, while the far-field radiation pattern is kept unchanged (i.e. zero-forward or zero-backward scattering). In addition, we derive the generalized “Brewster’s angles” for the spherically anisotropic particles. The high-quality polarized scattering wave

and the tunable polarization conversion can be achieved through the suitable adjustment of the electric and magnetic anisotropies. We hope our results will shed some light on both the theoretical and experimental study on the directionality of light scattering and the applications in high-quality linear polarizers.

Acknowledgments

This work was supported by the NNSF of China (No. 11074183), the National Basic Research Program (No. 2012CB921501), the Key Project in NSF of Jiangsu Education Committee (No. 10KJA140044), and PAPD of Jiangsu Higher Education Institutions. This work A.E. M. was supported by the Australian Research Council through the Future Fellowship program.